Multi-criteria Analysis of Five Reinforcement Options for Peruvian Confined Masonry Walls

Nicola Tarque*[1a], Jhoselyn Salsavilca [1b], Jhair Yacila[1c] and Guido Camata[2d]

[1]Pontificia Universidad Católica del Perú. Department of Civil Engineering. Grupo GERDIS-PUCP, San Miguel 15088, Lima, Peru
[2]University G.d'Annunzio of Chieti and Pescara. Department of Engineering and Geology. Pescara 65127, Italy

(Received keep as blank , Revised keep as blank , Accepted keep as blank)9pt

Abstract. In Peru, construction of dwellings using confined masonry walls (CM) has a high percentage of acceptance within many sectors of the population. It is estimated that only in Lima, 80% of the constructions use CM and at least 70% of these are informal constructions. This mean that they are built without proper technical advice and generally have a high seismic vulnerability. One way to reduce this vulnerability is by reinforcing the walls. However, despite the existence of some reinforcement methods in the market, not all of them can be applied massively because there are other parameters to take into account, as economical, criteria for seismic improvement, reinforcement ratio, etc. Therefore, in this paper the feasibility of using five reinforcement techniques has been studied and compared. These reinforcements are: welded mesh (WM), glass fiber reinforced polymer (GFRP), carbon fiber reinforced polymer (CFRP), steel bar wire mesh (CSM), steel reinforced grout (SRG). The Multi-Criteria Decision Making (MCDM) method can be useful to evaluate the most optimal strengthening technique for a fast, effective and massive use plan in Peru. The results of using MCDM with 10 criteria indicate that the Carbon Fiber Reinforced Polymer (CFRP) and Steel Reinforced Grout (SRG) methods are the most suitable for a massive reinforcement application in Lima.

Keywords: strengthening techniques, confined masonry, MCDM

1. Introduction

Confined masonry buildings are considered one of the most popular worldwide because of their easy and quick construction (Alcocer et al. 2003). Its use is common in Central and South America, Southeast Europe, India and other parts of Asia (Bhattacharya et al. 2013). For example, CM has been used in Chile and Colombia since the 1930's and in Mexico since the 1940's (Brzev and Perez 2014). According to Alcocer et al. (2003), until 2003, over 70% of Mexico's constructions made use of masonry. In Pakistan, 62.38% of all its buildings were constructed with masonry (Lodi et al. 2012), in some cities the percentage of masonry building stock could be even more than 90% (Ahmad et al. 2010). Peru is another case whose statistics (Fig. 1(a)) show that the predominant material of the houses' outer walls with 56% is brick or cement block, which are based for confined masonry buildings. It is worth pointing out that in Lima, capital of Peru, brick and cement block represent 82% of the materials in the houses' outer walls (INEI 2017, Lovon et al. 2018).

Corresponding author, Ph.D. Nicola Tarque, E-mail: sntarque@pucp.edu.pe
[a]Ph.D.,E-mail: sntarque@pucp.edu.pe
[b]Eng., E-mail: jsalsavilcap@pucp.pe
[c]Eng., E-mail: jhair.yacila@pucp.edu.pe
[d]Ph.D., E-mail: g.camata@unich.it

Considering that many of these countries, such as Peru, are located in high seismic activity zones, different seismic events have shown poor seismic performance of existing masonry structures built informally. Moreover, depending on the formality of the construction, quality of technical personnel, characteristics of the structure itself and other parameters; the seismic vulnerability associated with these constructions is high, which results in a high risk. Obviously, the seismic hazard can not be reduced; however, vulnerability can be reduced since it is associated with the intrinsic properties of the edification.

Therefore, it is evident the need for reducing the seismic vulnerability of informal masonry constructions. These steps consist of carrying out constant investigations about the possible repair and reinforcement systems for Peruvian confined masonry walls in order to enhance the seismic performance (Popa et al. 2016, Remki et al. 2016, Smyrou 2015, Srechai et al. 2017). Several studies in this field have already been carried out by different universities. In this paper, the studies carried out in the Pontificia Universidad Catolica del Peru (PUCP) are presented.

Some studies carried out in Peru about the most relevant reinforcement techniques use welded wire mesh reinforcement (San Bartolomé and Castro 2002, San Bartolomé et al. 2008), glass rod reinforced polymer (San Bartolomé and Loayza 2004), carbon fiber reinforced polymer (San Bartolomé and Coronel 2009), steel bar wire mesh (Luján and Tarque 2016), and galvanized steel fiber with natural lime mortar (SRG) (Salsavilca et al. 2019). Each

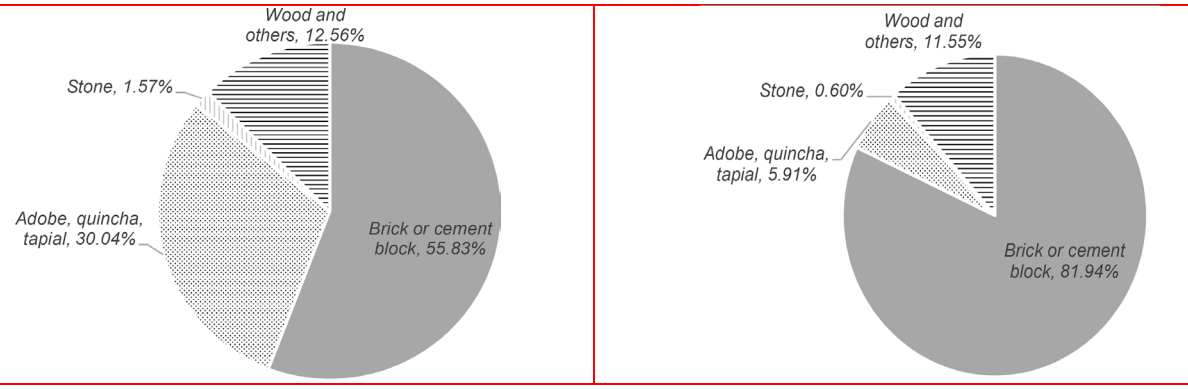

Fig. 1 Predominant material in the houses' outer walls in: (a)Peru, (b) Lima (INEI 2017)

of these reinforcements was applied to confined masonry walls on a natural scale, previously tested to their break strength or repair limit in the Structural Laboratory of the Pontificia Universidad Católica del Perú.

Although these techniques were already studied, the identification of a unique technique that allows for a fast, effective and massive application constitutes one of the main challenges faced by the academy. The decision making process becomes more complicated if many criteria are considered. For a fast application, duration and difficulty of application should be considered. For a massive use, the technique should meet cost-effectiveness requirements. For an effective technique, the seismic performance in terms of stiffness, load capacity and ductility must be evaluated. The efficacy of a reinforcing system depends also on its durability and compatibility with the strengthened substrate. The durability is crucial for the long-term effectiveness of the reinforcement (De Santis et al. 2017) under varying temperature, moisture and other environmental factors (Cabral et al. 2018). The compatibility property measures the effectiveness of two materials to work together. In case of strengthening techniques, there should be compatibility with thermal expansion coefficient and elastic modulus of substrate. It could be said that lime-based mortars which belong to SRG are mainly used for applications to historic substrates, needing relatively low Young's modulus to meet mechanical compatibility requirements (De Santis et al. 2017).

This work presents a summary of the previously mentioned investigations and identifies a reinforcement method through multi-criteria analysis using the MCDM TOPSIS method (Hwang and Yoon 1981). To identify the most suitable method, each reinforcement's characteristics and application process have been described. In addition, the improvement of earthquake-resistance properties of the walls such as stiffness, seismic capacity, and ductility, presented by each reinforcement method has been studied. The economic aspect is discussed in terms of labor and materials since this paper pretends to decide for one technique among the five ones in order to accomplish a massive use plan. It is worth mentioning that a mechanical ratio was taken into account as a main criteria in MCDM. This mechanical ratio gives an idea of how much quantity of reinforcement is needed in order to reach a certain strengthening capacity. Furthermore, aspects such as the duration of application, durability, compatibility, aesthetics, and initial test conditions are also considered.

According to the MCDM TOPSIS method, the best solutions for a fast, effective and massive application in Peru turned out to be the Carbon Fiber Reinforced Polymer (CFRP) and Steel Reinforced Grout (SRG).

2. Description of the five reinforcement options

2.1 Steel as reinforcement material: welded wire mesh and steel bar wire mesh

For a long time, in the area of the most studied reinforcement techniques, steel has been considered as a reinforcement material capable of reducing the damage in existing masonry structures. It has appeared as the main material in several reinforcement systems such as cladding, welded wire mesh, cable system, and steel bar wire mesh. The welded wire mesh technique (WM) basically consists of a set of deformed steel rods with a 4.5 mm diameter and spaced every 150 mm. This material is placed on both sides of the walls interconnecting them with #8 (4.2 mm diameter)

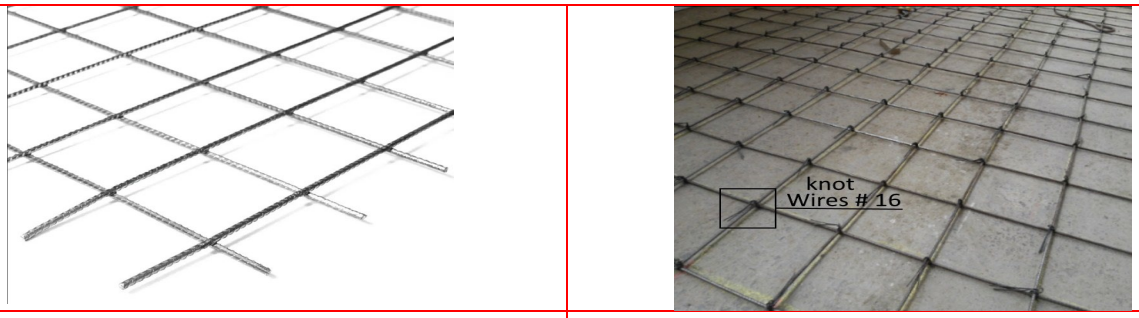

(a) (b)

Fig. 2 Steel as reinforcement material: (a) WM, (b) CSM

(a) (b)

Fig. 3. Reinforcement process for WM and CSM: (a) Mesh placed on wall's both sides, (b) Outer mortar layer covering the mesh

wires through previous perforations in the wall section. Then, the surface is plastered with mortar obtaining 25 mm of additional thickness on each side of the wall (Fig.3). On the other hand, the steel bar wire mesh technique (CSM) consists of preparing a mesh of steel rods with 4.7 mm diameter; the steel rods are connected with #16 (1.65 mm diameter) wires. The meshes are connected through previous perforations in the wall with #8 (4.2 mm diameter) wire and are tied against the knots of the meshes on both sides with #16 (1.65 mm diameter) wire. Same as the previous technique, the wall is plastered so that it does not exceed 25 mm on each side. The difference between both procedures lies in the making of the meshes, while the welded wire mesh is a prefabricated reinforcement, the steel bar wire mesh is made in-situ (see Fig.2).

2.2 FRP as a reinforcement system: carbon and glass fiber

This reinforcement system consists of high strength fibers impregnated in a polymer matrix (two component epoxy resin). It is recommended because of the excellent properties of its components such as glass, carbon, basalt fibers among others (Buchan and Chen 2007). This section presents the CFRP and GFRP (carbon fiber reinforced polymer and glass fiber reinforced polymer) as reinforcement techniques with higher tensile mechanical characteristics due to them being discontinuous phase materials (Corradi et al. 2002).

Both CFRP and GFRP are easy and quick to apply. The CFRP system is made up of a light and high resistance unidirectional carbon fiber sheet (surface density = 3 x 10^{-10} *tonne/mm*^{2}) that is embedded in three types of resins. The CFRP system consists of applying the first epoxy compound (that works as a primer to seal the pores) on the masonry surface and another epoxy paste (putty) to level the surface. Then, the carbon fiber is placed so that it is finally coated by the third type of epoxy resin (saturant) that encapsulates the fibers. The final sketch for the studied wall is shown in Fig.4(a). The GFRP system is made up of glass fibers impregnated with vinyl ester resin. They are deformed and covered with a layer of fine sand. They are not electrically conductive and are very light (g = 2.26 x 10^{-9} *tonne/mm*^{3}). This GFRP system basically consists of installing the glass fiber rods as interior horizontal reinforcement every 2 rows of bricks, interspersed alternately on both sides of the wall in order to avoid weakening the cross section of the reinforced wall (see Fig.4(b)).

Table 1 lists characteristic values for the fibers used in the past experimental investigations (San Bartolomé and Loayza 2004, San Bartolomé and Coronel 2009).

2.3 SRG as a reinforcement system: galvanized steel fiber

Currently, other reinforcement options such as the Fabric Reinforced Cementitious Matrix (FRCM), Fiber Reinforced Matrix (FRM), Steel Reinforced Grout (SRG) have arisen to compete against the previous ones, given the advantages offered by the inorganic matrix that composes them. This results in a high resistance to fire and UV rays protection.

Moreover, the use of inorganic mortars allows a better adhesion to a non-uniform surface such as masonry (Gattesco and Boem 2017). Consequently, FRMs draw attention due to their application to historical structures (Ghiassi et al. 2016). The SRG (Steel Reinforced Grout) system is made up of UHTSS (Ultra High Tensile Strength Steel) and natural lime mortar. The fiber used was galvanized steel coated with zinc. This mesh is unidirectional and consists of strings that are

(a) (b)

Fig. 4 FRP as reinforcement system: (a) Carbon, (b) Glass

Table 1 Mechanical properties of the strengthening systems

		Carbon Fiber	Glass fiber rods	Galvanized steel	Lime-based mortar
Tensile Strength	[MPa]	3800	827	2861	2.92*
Compressive Strength	[MPa]	-	-	-	22
Young's Modulus	[GPa]	227	40.7	157	9.1
Elongation at failure	[%]	1.67	0.16	2.44	-
Equivalent thickness/Diameter	[mm]	0.165	6.25	0.084	-

*Carloni (2017)

obtained by twisting two wires around three rectilinear ones (see Fig. 5(a)). In addition, the mortar that works as binding is made of lime with type M15 resistance according to the EN 998-2 and type R1 according to EN 1504-3.

Previous researches (Salsavilca et al. 2019, Yacila et al. 2019, Carloni 2017) have characterized the materials of SRG and Table 1 shows the characteristic values of the materials that were used.

This technique is quite easy to apply, so it does not need experts. Before applying SRG, several aspects must be taken into consideration, such as wall clearance, strip clearance, mortar preparation, compound application and curing. Thus, after treating the surface by removing the dust and dampening it, a first layer of 5 mm mortar is applied. Then, the mesh is placed manually and pressed on the fresh mortar in order to then apply a second layer of mortar 5 mm thick. In this way, it is obtained 10 mm of additional thickness on each side of the wall. Finally, unlike other type of reinforcements, it is cured by moistening the walls directly with water 3 times a day for 7 days.

The good performance of SRG system has turned out to be substantially dependent on the bond behavior between the composite layer and the substrate. Salsavilca et al. (2019) evaluated the bond behavior between SRG and masonry, and the average ultimate stress was equal to 1738 MPa.

Additionally, De Santis et al. (2017), by means of experimental tests on SRG, pointed out an average tensile strength equal to 2838 MPa.

3. Experimental Campaign

As follows, the results of five experimental campaign done by different authors at the PUCP are summarized and compared between them in terms of in-plane Force F vs Displacement D curve. The geometry, dimension and mechanical characteristics of each wall is presented in Fig. 6 and Table 2. In all tests, the masonry wall was subjected to in-plane cyclic loading up to a specific drift. Then, the walls were repaired and strengthened. Finally, the walls were tested again up to the ultimate limit state. Just the wall with SRG was tested without and with reinforcement up to the ultimate limit state in both cases. All the studies were performed in full-scale confined masonry walls with a stretcher bond. The column-masonry joint used by San Bartolomé and Loayza (2004) and San Bartolomé and Coronel (2009) was flush, while the rest of investigations (3) presented a toothed connection (see Fig 6).

3.1 Characteristics of specimens

The masonry unit used in each investigation was solid (percentage of void less than or equal to 30%) or hollow (percentage of voids greater than 30%), which directly influences the masonry axial compressive strength (f_m) and shear resistance (v_m) as shown in Table 2. The properties of the masonry such as compressive strength (f_m) and modulus of elasticity (E_m) were obtained by performing an axial compression test, and the shear strength (v_m) was obtained by performing the diagonal compression test. Both control tests were performed on piles and walls, respectively. Table 2 shows the mechanical properties extracted from cited investigations, except for the first three values of E(*) that were calculated according to the NTP E.070 (2006) that estimates E = 500 f_m.

It is worth mentioning the configuration adopted for each wall during the strengthening process since the quantity of reinforcement material influences on the final load-displacement response. In case of the welded mesh technique, it was used a mesh that covered both sides of the wall. This grid was comprised of bars (diameter 4.5 mm) spaced 150 mm vertically and horizontally. In the GFRP strengthened wall, five glass rods were place on each side with a spacing equal to 400 mm (see Fig. 4(b)). For CFRP

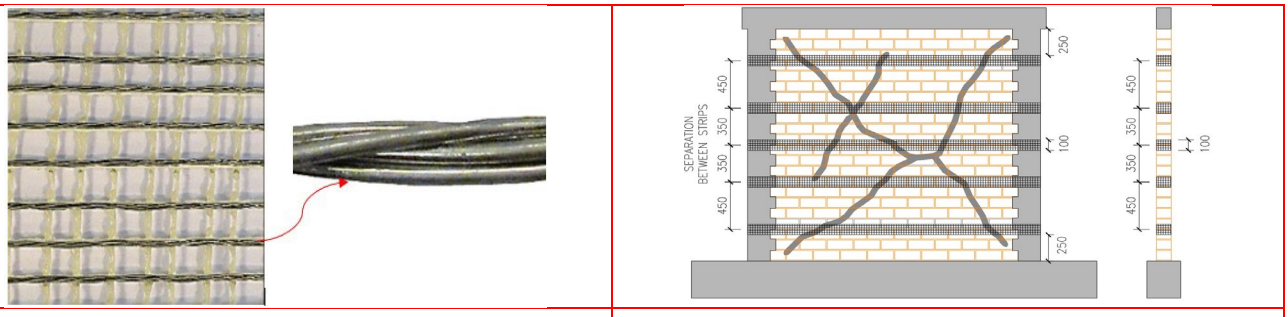

(a) (b)

Fig. 5 (a) Steel Galvanized Fiber ((De Santis *et al.* 2017)), (b) sketch of SRG strengthened wall

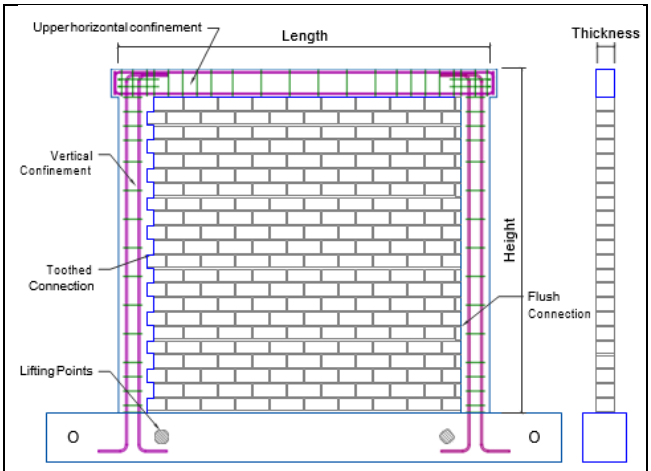

Fig. 6 Sketch of tested walls

technique, it was computed that seven strips with a width of 100 mm will carry the load imposed during the cyclic test. Four strips were place on one side and the remaining in the other side with an approximated spacing of 600 mm (see Fig. 4(a)). The wall reinforced with CSM had a configuration similar to WM since the bars (diameter 4.7 mm) were spaced 150 mm vertically and horizontally. Finally, the sketch of the wall strengthened with SRG comprised of five strips around all the wall. The strips width was 100 mm and the space between strips was approximated 400 mm (see Fig. 5(b)).

Similarly, it should be pointed out the additional thickness that each strengthening technique provides to the wall since it is an aspect that influences on the stiffness recovering besides the reparation process which is so important too. Traditional techniques as WM and CSM add 25 mm to each entire side of the wall. Innovative techniques as GFRP do not add thickness since fiberglass rods are inside every 2 bed mortar joints, CFRP adds around 4 mm considering the epoxy resin and fiber, and SRG adds approximated 10 mm to each strengthened strip of the wall.

3.2 Test Protocol

The test carried out on the walls was a lateral in-plane cyclic loading test with controlled horizontal displacement (pseudo-static test) with no vertical load, which results in a wall with a lower lateral stiffness compared to a wall with vertical load. The lateral load was applied at a rate of 1 cycle in 4 minutes. Fig. 7 shows the typical test scheme for all the studied walls. The instrumentation of the tests consisted of the following equipment: (1) dynamic actuator, (2) hydraulic jack and (3) steel beam.

The displacements were imposed by the dynamic actuator that had an internal LVDT for proper displacement control. This actuator was attached to the reaction frame, which was assumed to be a fixed structure. Thus, the idea was to obtain the relative displacements of the walls with respect to a point of the reaction frame. The objective of the tests was to determine the improvement of seismic behavior in strengthened walls and measure its resistance, stiffness and ductility variation.

A typical displacement history is plotted in Fig. 8 and Table 3 shows the displacement history according to each type of reinforcement studied. In the case of the welded wire mesh (WM), the wall without reinforcement was subjected to 7 phases until a maximum lateral displacement of 12.5 mm (0.52 % drift) was reached. The reinforced wall was subjected to 9 phases until a maximum lateral displacement of 17.5 mm (0.73 % drift) was reached. For the glass fiber reinforced polymer (GFRP), the wall with and without reinforcement was subjected to 10 phases until a maximum lateral displacement of 20.0 mm (0.77%drift) was reached. For the carbon fiber reinforced polymer (CFRP), the wall without reinforcement was subjected to 8 phases until a maximum lateral displacement of 15.0 mm (0.58%drift) was reached. The reinforced wall was subjected to 11 phases until a maximum lateral displacement of 25.0 mm (0.96 % drift) was reached. The displacement history for the last two CSM and SRG studies complied with the guidelines of FEMA 461 (2009), which establishes that the displacements for each superior phase must be the result of increasing the immediate inferior displacement by a factor of 1.4 times. Then, for the deformed steel mesh (CSM), the wall without reinforcement was subjected to 11 phases until a maximum lateral displacement of 20.0 mm (0.83 % drift) was reached. The reinforced wall was subjected to 12 phases until a maximum lateral displacement of 26.0 mm (1.08 % drift) was reached. Finally, for the galvanized steel fiber reinforced wall (SRG), the wall without reinforcement was subjected to 11 phases until a maximum lateral displacement of 20.0 mm (0.83 % drift) was reached. The reinforced wall was subjected to 12 phases until a maximum lateral displacement of 30.0 mm (1.25 % drift) was reached.

3.3 Results for walls with and without reinforcement

3.3.1 Welded Wire Mesh (WM)

All walls were preliminary tested until a specific drift and then repaired, strengthened and tested again until the wall collapse. In this case, the unreinforced wall failed due to shear stress, while the strengthened wall failed due to bending stress. This is because the welded wire mesh was able to restraint, to a large extent, the opening of the repaired cracks. The first cracks due to bending appeared in the base

Table 2 Mechanical and geometric properties of walls studied

Strengthening Technique	Masonry Unit (voids %)	*fm* [Mpa]	*Em* [Gpa]	*vm* [Mpa]	L [mm]	H [mm]	t [mm]	H/L
Welded Mesh (WM)	Solid (30)	8.6	4555*	1.67	2600	2400	130	0.92
Fiber Glass Rod (GFRP)	Hollow (45)	12.7	6726*	1.57	2400	2680	130	1.08
Carbon Fiber Mesh (CFRP)	Solid (32)	8.8	4661*	0.94	2400	2600	130	1.00
Corrugated Steel Mesh (CSM)	Hollow (48)	9.46	5010	1.25	2600	2400	130	0.92
Steel Reinforced Grout (SRG)	Hollow (48)	9.46	5010	1.25	2600	2400	130	0.92

L= length, H= height, t= thickness

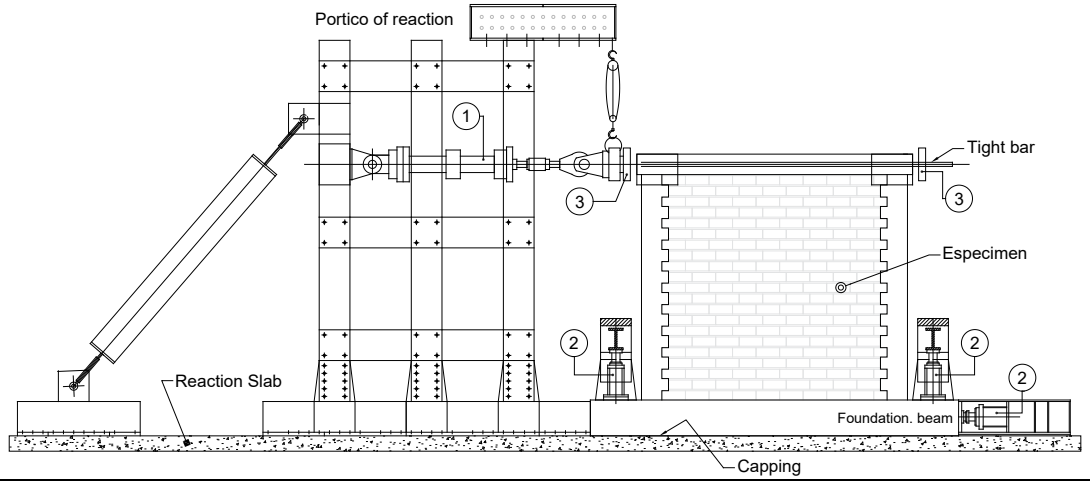

Fig. 7 Assembly for tests of confined masonry walls

of the columns at a 0.04% drift. Then, at a 0.21% drift, occurred the first crack due to shear stress, characterized by a diagonal crack in the masonry panel. Later, at a 0.42% drift, the bricks in the lower corners of the walls crushed. Finally, at a 0.52% drift, the top beam-column joints failed. Fig. 9 shows the failure pattern for original and strengthened walls, where it can be seen that during the second test, the preliminary repaired cracks re-open again, but without increasing the crack thickness. Also, new cracks appear in the wall. In this case the WM helped the wall to develop more thinner cracks. In Fig. 9(a) the connection with wall and column was toothed connection. In Fig. 9(b) the same wall was strengthened and covered by cement plaster.

In terms of the strengthened wall, at a 0.04% drift, the first cracks due to bending appeared in the lower zones of the columns. Then, at a 0.10% drift, diagonal cracks due to shear stress were observed. These cracks were very thin because the welded wire mesh controlled the thickness. Later, at 0.31% drift, new cracks appeared at the base of the columns. At a 0.52% drift, a sliding failure started to develop in the base of the wall. In addition, a vertical crack was generated in the lower part of the masonry-column joint because the mesh was not connected to the columns.

The initial stiffness of the strengthened wall reached 89% of the initial stiffness of the wall. Likewise, the initial stiffness of the strengthened wall resulted in an increase of 8 times the final stiffness of the original wall. Fig. 10 shows the comparison in the hysteresis loops envelopes of both walls, original and strengthened. From Fig. 10, it can be seen that the welded wire mesh reinforcement was able to increase the load capacity of the original wall by a 38% and the ductility by a 40% as well.

3.3.2 Glass Fiber Reinforced Polymer (GFRP)

At a 0.10% drift, the first crack due to bending tensile stress appeared in the tie-column, while at a 0.19% drift, the existing cracks in the tie-columns spread to the interior of the masonry panel diagonally. Then, at a 0.29% drift, new diagonal cracks formed in the panel. In phases 6, 7 and 8 (drifts equal to 0.38%, 0.48% and 0.58%, respectively), these diagonal cracks intensified with the presence of the crushing of 2 bricks in the central part of the wall. Finally, at a 0.77% drift, the diagonal cracks spread towards the tie-columns. Fig. 11 shows the failure pattern for both walls, original and strengthened.

In the case of the strengthened wall, the first cracks in the masonry panel were observed at a 0.04% drift. At a 0.10% drift, the first cracks due to bending stress appeared in both tie- columns. At a 0.19% drift, very thin diagonal cracks appeared. For a 0.29% drift, the fixed cracks started opening. For a 0.38% drift, the thickness of the cracks due to shear stress (i.e. diagonal cracks) was controlled by the GFRP rods. For a 0.48% drift, cracks additional to those of the original wall were formed, and at a 0.58% drift, the central GFRP rod

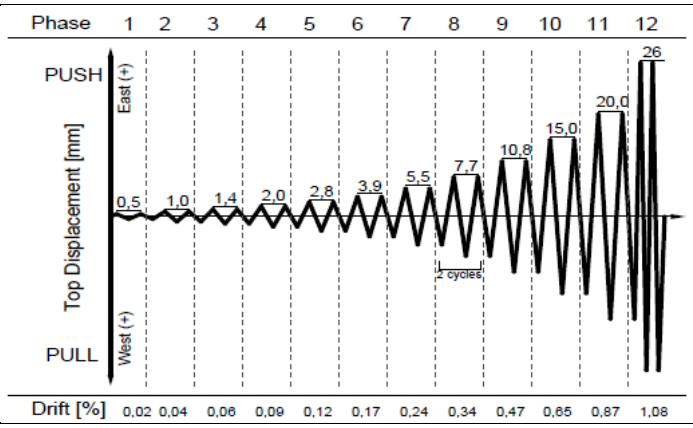

Fig. 8 Typical Displacement History

Table 3 Phases of quasi–static test for walls with and without reinforcement

Technique	Concept	Protocol											
WM	Phase	1	2	3	4	5	6	7	8	9			
	Disp. [mm]	0.5	1.0	2.5	5.0	7.5	10.0	12.5	15.0	17.5			
	Drift [%]	0.02	0.04	0.10	0.21	0.31	0.42	0.52	0.63	0.73			
	Cycles	1	1	2	2	2	2	2	3	3			
GFRP	Phase	1	2	3	4	5	6	7	8	9	10		
	Disp. [mm]	0.5	1.0	2.5	5.0	7.5	10.0	12.5	15.0	17.5	20.0		
	Drift [%]	0.02	0.04	0.10	0.19	0.29	0.38	0.48	0.58	0.67	0.77		
	Cycles	1	1	2	2	2	2	2	3	3	3		
CFRP	Phase	1	2	3	4	5	6	7	8	9	10	11	
	Disp. [mm]	0.5	1.0	2.5	5.0	7.5	10.0	12.5	15.0	17.5	20.0	25.0	
	Drift [%]	0.02	0.04	0.10	0.19	0.29	0.38	0.48	0.58	0.67	0.77	0.96	
	Cycles	2	1	2	3	3	3	3	3	3	3	1	
CSM	Phase	1	2	3	4	5	6	7	8	9	10	11	12
	Disp. [mm]	0.5	1.0	1.4	2.0	2.8	3.9	5.5	7.7	10.8	15.0	20.0	26.0
	Drift [%]	0.02	0.04	0.06	0.08	0.12	0.16	0.23	0.32	0.45	0.63	0.83	1.08
	Cycles	2	2	2	2	2	2	2	2	2	2	2	2
SRG	Phase	1	2	3	4	5	6	7	8	9	10	11	12
	Disp. [mm]	0.5	1.0	1.4	2.0	2.8	3.9	5.5	7.7	10.8	15.0	20.0	30.0
	Drift [%]	0.02	0.04	0.06	0.08	0.12	0.16	0.23	0.32	0.45	0.63	0.83	1.25
	Cycles	2	2	2	2	2	2	2	2	2	2	2	1

was exposed in its middle part. For a 0.67% drift, the GFRP rods started to buckle in several areas of the wall. Finally, at a 0.77% drift, the central part of the wall was crushed and the GFRP rods started losing adhesion with the masonry.

The initial stiffness of the strengthened wall reached 57% of the initial stiffness of the original wall. Likewise, the initial stiffness of the strengthened wall resulted in an increase of 5.8 times the final stiffness of the original wall. Fig. 12 shows the comparison in the envelopes of hysteresis loops of both walls, original and strengthened. From Fig. 12, it can be inferred that the glass fiber reinforcement was able to increase the loading capacity of the original wall only by 3% and was not able to increase the ductility of the system.

(a) Original

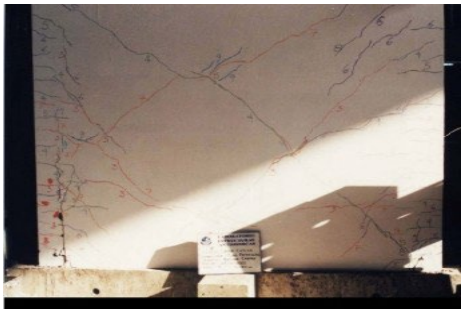

(b) Strengthened

Fig. 9 Strengthening with welded mesh WM

3.3.3 Carbon fiber reinforced polymer (CFRP)

During the test on the original wall, there were no cracks up until a 0.10% drift, when the first diagonal crack appeared in the lower half of the masonry. Similarly, there were bending stress cracks in both tie-columns. At a 0.19% drift, 2 diagonal cracks appeared throughout the wall. At a 0.48% drift, the masonry in the intersection of the diagonal cracks started being crushed. Finally, at a 0.58% drift, the lower edge of one of the tie-columns was completely crushed. Fig. 13 shows the failure pattern for original and strengthened walls.

In the reinforced wall, the diagonal cracks started in the upper center of the wall, at a 0.10% drift. During phases 4, 5, 6 and 7 (drift = 0.19%, 0.29%, 0.38% and 0.48%, respectively), the diagonal cracks continued to extend throughout the masonry panel. At a 0.58% drift, one of the bands located in the center of the wall suffered a small rupture. At a 0.67% drift, the band finished breaking. At a 0.77% drift, rupture and partial detachment of other bands occurred. Finally, at a 0.96%, the reinforced wall failed with

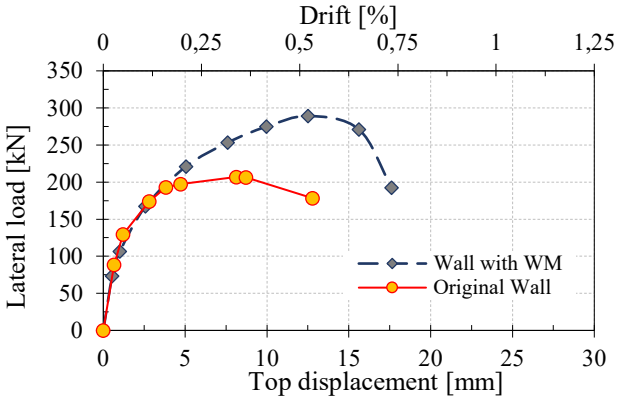

Fig. 10 Envelopes of hysteretic loops on walls with and without reinforcement WM

rupture and partial detachment of other bands. The upper bands remained in good condition.

The initial stiffness of the strengthened wall reached 53% of the initial stiffness of the original wall. Similarly, the initial stiffness of the strengthened wall resulted in an increase of 12.4 times the final stiffness of the original wall. Fig. 14 shows the comparison in the envelopes of hysteresis loops of both walls, original and strengthened. From Fig. 14, it is inferred that the carbon fiber reinforcement was able to increase the loading capacity of the original wall by 20% and the ductility by 67%.

(a) Original

(b) Strengthened

Fig. 11 Strengthening with GFRP. See Fig. 4(b) to see where the GFRP was placed in the wall.

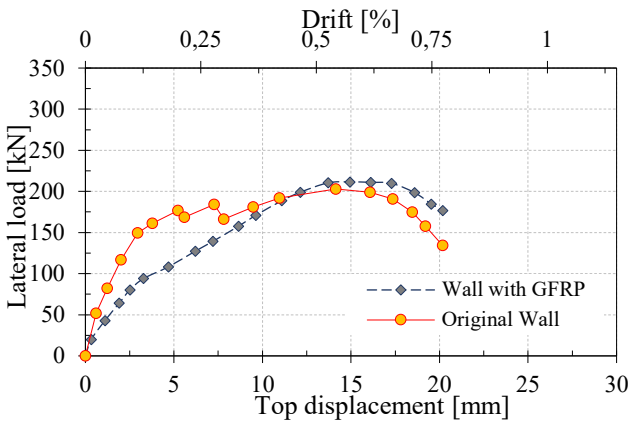

Fig. 12 Envelopes of hysteretic loops on walls with and without reinforcement GFRP

3.3.4 Deformed steel mesh (CSM)

The first cracks, on the original wall, occurred at a 0.04% drift and were due to bending stress in the tie-columns. In phase 3 and 4 (drift = 0.06% and 0.08%, respectively) fine cracks started to appear in the masonry panel. At a 0.12% drift, stepped cracks appeared on the lower part of the panel. In phase 6 and 7 (drift = 0.16% and 0.23%, respectively), new cracks started to form in the upper corners of the wall. During phase 8 and 9 (drift = 0.32% and 0.45%, respectively), the first diagonal cracks started to appear in the panel. Finally, in phases 10 and 11 (drift = 0.63% and 0.83%, respectively), some masonry areas were detached due to crushing, while the diagonal cracks intensified. Fig. 15 shows the failure pattern for both walls, original and strengthened.

For the strengthened wall, the first cracks appeared at a 0.04% drift and were due to bending stress in the tie-columns. At a 0.16% drift, the first diagonal, stepped, cracks appeared on the masonry panel. At a 0.23% drift, quite a few cracks appeared from the corners of the wall. At a 0.45% drift, two diagonal v-shaped cracks formed up to the lower part of the wall. During phases 10 and 11 (drift = 0.63% and 0.83%, respectively), the number of cracks was not increased, but rather the existing ones became more pronounced.

The stiffness of the strengthened wall reached 86% of the initial stiffness of the original wall. Similarly, the initial stiffness of the strengthened wall resulted in an increase of 6.5 times the final stiffness of the original wall. Fig. 16 shows the comparison of envelopes of hysteresis loops for both walls, original and strengthened. From Fig. 16 can be inferred that the deformed steel mesh reinforcement was able to increase the loading capacity of the original wall by 21% and the ductility by 25%.

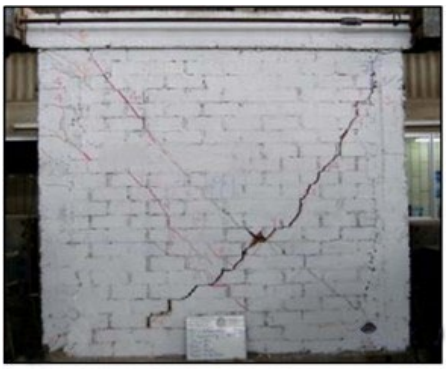

(a) Original

(b) Strengthened

Fig. 13 Strengthening with CFRP. See Fig. 4(a) to see the zones were the CFRP was placed in the wall.

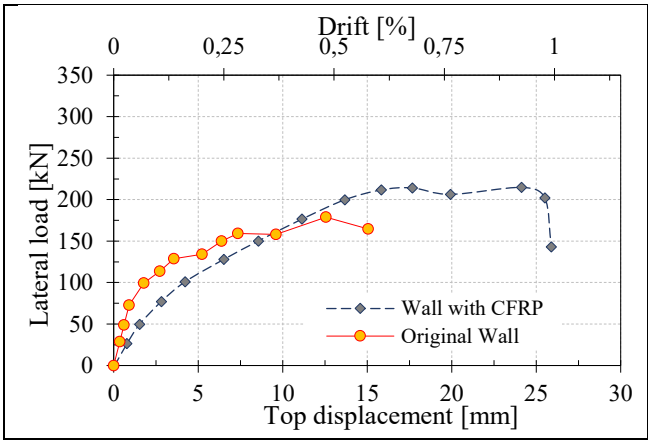

Fig. 14 Envelopes of hysteretic loops on walls with and without reinforcement CFRP

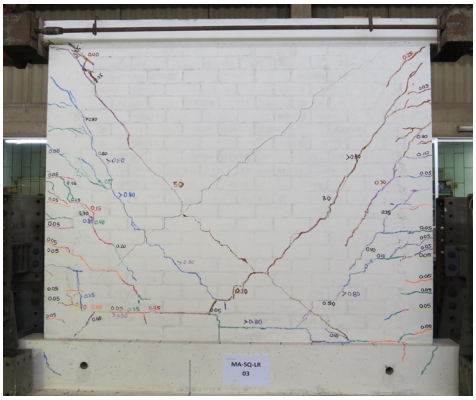

(a) Original

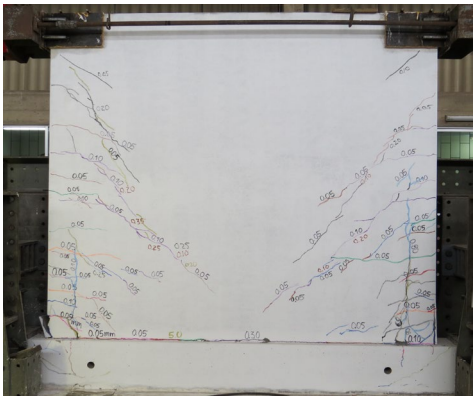

(b) Strengthened

Fig. 15 Strengthening with CSM

3.3.5 Galvanized steel fiber (SRG)

The first cracks, on the original wall, occurred at a 0.04% drift and were due to bending stress in the tie-columns. At a 0.08% drift, some of the cracks generated by bending stress in the lower part of the columns started to spread diagonally on the masonry panel. At a 0.12% drift, a horizontal crack appeared in the lower part of the masonry panel. At a 0.16%

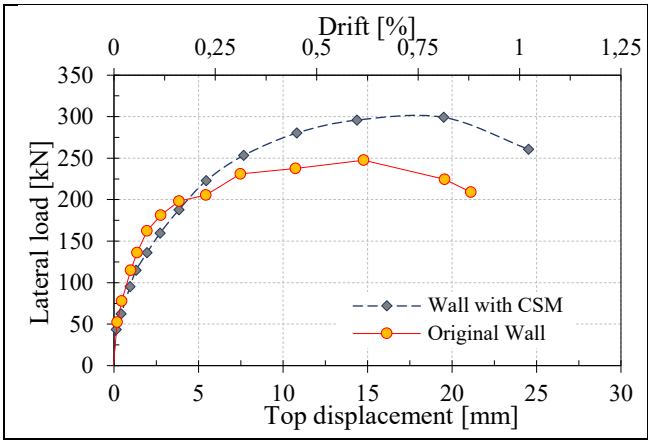

Fig. 16 Envelopes of hysteretic loops on walls with and without reinforcement CSM

drift, new diagonal cracks started forming from the upper corners of the wall. At a 0.23% drift, two of the diagonal cracks were intercepted in the lower part of the wall forming a V shape. In phases 8, 9 and 10 (drift = 0.32%, 0.45% and 0.63%, respectively), no new cracks appeared, but the existing ones intensified. Finally, at a 0.83% drift, a new fissure, not very long, appeared in the lower part of the wall.

According to the evolution of cracks, although there were diagonal cracks, these were the result of the spreading of smaller cracks produced in previous phases, which is not typical of a failure by shear stress. Therefore, a failure of the wall by bending tress was predominant. Fig. 17 shows the failure pattern for both walls, original and strengthened.

(a) Original

(b) Strengthened

Fig. 17 Strengthening with SRG

The first cracks of the strengthened wall occurred at a 0.04% drift and were due to bending stress in the tie-columns. In phases 4 and 5 (drift = 0.08% and 0.12%, respectively) diagonal cracks started to appear on the masonry panel, at low and high heights, from the joint of the columns with the masonry towards the center of the wall. Some of them corresponded to the opening of repaired cracks of the original wall. At a 0.16% drift, no new cracks appeared, but the already existing ones intensified. At a 0.23% drift, two of the diagonal cracks intercepted on the lower part of the masonry panel, forming a V shape. Like the original wall, this is due to a generalized failure by bending stress in the strengthened wall. In phase 8, at a 0.32% drift, a new, not very long, diagonal crack appeared on the masonry panel from the upper corner towards the center of the wall. From phase 9 (drift = 0.45%), the opening of cracks started causing the surface detachment of the masonry. In phase 11, at a 0.83% drift, a new diagonal crack appeared in the opposite direction to the one mentioned in phase 8. This crack was indeed generated along one of the diagonals of the wall, so it is associated to a failure by shear stress. Finally, at a 1.25% drift, the diagonal cracks, generated in phases 8 and 11, intercepted forming an X shape.

The stiffness of the strengthened wall reached 55% of the initial stiffness of the original wall. Similarly, the stiffness of the strengthened wall resulted in an increase of 8.4 times the final stiffness of the original wall. Fig. 18 shows the comparison of envelopes of hysteresis loops of both walls, original and strengthened. From Fig. 18 can be inferred that the deformed steel mesh reinforcement was able to increase loading capacity of the wall only by 4% and the ductility by 50%.

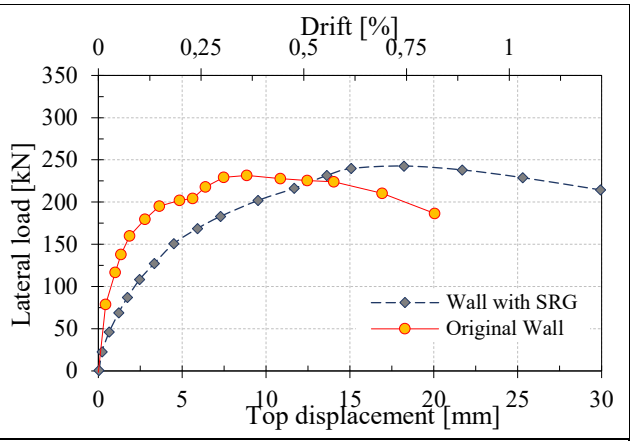

Fig. 18 Envelopes of hysteretic loops on walls with and without reinforcement SRG

4. Seismic Performance of the alternatives

The idea of reinforcing a structural element comes from trying to restore o increase some of its seismic resistance parameters. As shown in the item before, the more relevant effects of using a reinforcing technique can be to restore the initial stiffness, or a good percentage of the same, to regain the load capacity or gain a greater one, to show a greater ductility, or just develop a combination of these. To restore the initial stiffness will help the wall receive once again the same seismic load that led to its collapse. A greater load capacity will allow the wall to have a greater resistance to the displacements imposed by an earthquake. A greater ductility will help the wall dissipate larger seismic energy, which in turn will help reduce the damage in vulnerable structural elements. It is important to ascertain the right combination of parameters for each building.

There are several factors that can influence the response of the wall, some of them have been shown in Table 2, such as the type of unit employed in the construction of the walls, the axial compression strength f_m in masonry, as well as the shear strength v_m. Also, another factor that directly influences the response of the wall is the *H/L* ratio. It was observed that all the walls show almost the same geometry, therefore, this factor does not imply that there exists a high level of dispersion in the responses of the walls tested. Additionally, each wall presented different methods to connect confinement elements and masonry panel, and presented different quantity of reinforcement as was mentioned in Section 3.1. Moreover, in this same section, the reinforcement configuration of each technique which leads to different quantity of reinforcement material and the additional thickness that each technique provides to the wall were also discussed as wall's characteristics that influence on its final behavior. Finally, it is worth highlighting that the initial condition of the strengthened walls testing, i.e. not all original walls were tested until the same drift, affects the final response of each wall favoring some and others not. For instance, SRG wall was tested until the failure (drift=0.83%) while WM wall was tested until a drift equal to 0.52%.

The aforementioned characteristics of the walls imply that the strengthening techniques showed in this work can not be compared directly. Hence, a multi-criteria decision making (MCDM) for a massive seismic retrofitting of masonry walls was done in Section 6. Within MCDM approach, a technical effectiveness was taken account thus Table 4 shows the improvement in terms of initial stiffness (K_0), load capacity (P_{max}), ductility in terms of maximum displacement (d) for each reinforcement technique at failure strength. It is worth pointing out that the initial stiffness was computed in the third phase for each case in order to have a representative value due to a possible adjustment of instrumentation during the first phases. From Table 4, it is noted that WM and CSM techniques recovered approximated an 87% of the initial stiffness but much of this is due to the reparation process and the remaining is due to these techniques which increase 5 cm the total thickness of the wall. Techniques as GFRP, CFRP and SRG recovered approximated 55% of the initial stiffness, which can be attributed almost in total to the reparation process since these techniques almost do not increase wall's thickness. The seismic retrofitting needs to be also evaluated looking at the displacement ductility. It is important not to have fragile structures. Then, the CFRP, WM, and SRG shows an increment in the displacement ductility greater than 140%.

Since the quantity of reinforcement is different and some walls were built with hollow units and others with solid units, it is crucial to understand the influence that both factors may entail in the final load-response considering maximum

Table 4 Comparison of earthquake–resistant parameters of walls with and without reinforcement

Technique	Parameter	Original [O]	Drift	Reinforced [R]	Drift	Ratio [R/O]
WM	K_0 [kN/mm]	97.00		86.30		89%
	P_{max} [kN]	208.40	0.33%	286.90	0.52%	138%
	δ [mm]	12.50	0.52%	17.50	0.73%	140%
GFRP	K_0 [kN/mm]	63.20		36.00		57%
	P_{max} [kN]	203.10	0.58%	209.90	0.67%	103%
	δ [mm]	20.00	0.83%	20.00	0.83%	100%
CFRP	K_0 [kN/mm]	62.50		33.00		53%
	P_{max} [kN]	177.80	0.52%	213.60	0.74%	120%
	δ [mm]	15.00	0.63%	25.00	1.04%	167%
CSM	K_0 [kN/mm]	96.80		83.60		86%
	P_{max} [kN]	246.60	0.61%	298.00	0.83%	121%
	δ [mm]	20.00	0.83%	25.00	1.04%	125%
SRG	K_0 [kN/mm]	98.30		54.10		55%
	P_{max} [kN]	230.60	0.37%	240.90	0.76%	104%
	δ [mm]	20.00	0.83%	30.00	1.25%	150%

strength of the strengthened element and of the reinforcing material. Hereafter, a mechanical ratio can be calculated as follows:

$$\omega = \frac{A_s . f_s}{v_m . b . s} \quad (1)$$

where A_s represents the area of the strengthening material, f_s is the experimental tensile strength of the reinforcement system, v_m is equal to the experimental shear strength of masonry, s is the space between reinforcing materials of width b. Table 5 lists the mechanical ratios. It is observed that CFRP and SRG have lower values than WM, GFRP and CSM which means that even with less quantity of material of a certain tensile strength. Thus, a technically effective reinforcing system with a low value of **ω** is the best option.

Table 5 Mechanical ratio for strengthening techniques

	WM	GFRP	CFRP	CSM	SRG
A_s [mm^2]	44.98	61.36	33.00	49.07	16.08
f_s [MPa]	600	827	3800	618	2838
v_m [MPa]	1.67	1.57	0.92	1.25	1.25
b [mm]	4.50	6.25	100	4.70	100
s [mm]	150	400	585	150	400
ω	23.94	12.93	2.27	34.41	0.95

5. Cost-effectiveness of the alternatives

For the economical aspect, the cost of construction, repair and reinforcement in both sides of a typical CM wall were considered (see Table 6). Even though the construction and repair cost are independent from the reinforcing technique, they are being considered in order to have an idea of ratio of the repair and reinforcement cost against the construction. In addition, economical aspect is important since this paper pretends to recommend a strengthening technique able to be applied massively. Each process includes the cost of materials and labor.

The cost of materials and labor were calculated taking into account the actual Peruvian market at November 2018.

From Fig. 19, the percentage of repairing and strengthening over the construction for each wall is compared. If a cracked wall needs to be repaired and strengthened, then the materials and labor costs with WM represents 74%, GFRP 45%, CFRP 79%, CSM 76% and SRG 92% of the cost of a new wall, Fig. 19(a). However, if an intact wall needs to be just strengthened, then just the reinforcement cost over the construction' cost of a new wall results in 53% for WM, 24% for GFRP, 58% for CFRP, 55% for CSM and 71% for SRG, Fig. 19(b). It is worth noting that the difference is due to the labor cost for repairing.

Table 6 Costs summary for each technique (price in USD for a wall of 2.4 x 2.4m^2)

Technique	Construction (C) [$]	Reparation (R) [$]	Strengthening (S) [$]
WM	**462.00**	**98.00**	**248.00**
Materials	277.00	5.00	117.00
Labor	185.00	93.00	131.00
GFRP	**462.00**	**98.00**	**114.00**
Materials	277.00	5.00	61.00
Labor	185.00	93.00	53.00
CFRP	**462.00**	**98.00**	**267.00**
Materials	277.00	5.00	162.00
Labor	185.00	93.00	105.00
CSM	**462.00**	**98.00**	**254.00**
Materials	277.00	5.00	97.00
Labor	185.00	93.00	157.00
SRG	**462.00**	**98.00**	**328.00**
Materials	277.00	5.00	275.00
Labor	185.00	93.00	53.00

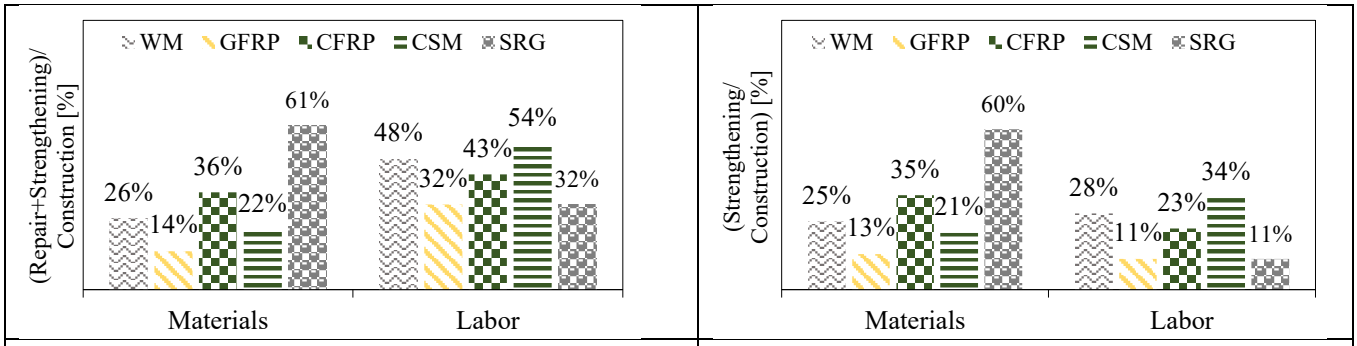

Fig. 19 Incidence of (a) repairing + strengthening costs and (b) strengthening cost over the cost of a new wall

It must be noted that before reinforcing new walls, it is required a technical evaluation of the most vulnerable walls against a seismic event. It is not necessary to reinforce all the walls of a building. Additionally, the reinforcement techniques have shown an improvement in the seismic-resistant parameters of the CM walls, however, they must be properly applied. Therefore, the personnel in charge of reinforcement should have been properly trained.

6. Multicriteria decision analysis

In Section 4 and 5, a technical and economical evaluation for each strengthening technique were presented, however, based on the results, it is not easy to decide which option is the best for a massive use in Peru. Multi-Criteria Decision Making (MCDM) methods are commonly employed to solve similar problems occurring in several fields (i.e. natural resources management, medical treatment choices, resources allocation planning) (Caterino et al. 2006). MCDM evaluates multiple conflicting criteria in decision making. As follows, the application of the MCDM TOPSIS (Technique for Order Preference by Similarity to Ideal Solution) method (Hwang and Yoon 1981) for the reinforcement of Peruvian confined masonry is discussed.

The criteria taken into account are stiffness (C_1), strength (C_2), ductility (C_3), mechanical ratio (C_4), installation cost (C_5), total cost (C_6), duration of application (C_7), aesthetics (C_8), durability (C_9), compatibility (C_{10}), and the initial test condition in regards of drift (C_{11}). The last parameter C_{11} follows the criterion of considering that not all the walls were brought to a reparability limit before being repaired and strengthened. Finally, it is worth mentioning that despite this research considers some tests on solid units and some other tests on hollow units, the multi-criteria analysis is still valid since these differences are taken into account in the mechanical ratio through the shear strength v_m of the masonry.

6.1 Importance of each criterion

In order to take into account the relative importance of each criterion, the definition of the weight w_i is needed, which references to the criterion C_i. The method used here is based in eigenvalue's theory (Saaty 1994) and allows calculating the weights as the eigenvalues of the matrix A.

This matrix is composed by a_{ij} components, and each component is the relative importance of the Ci criteria in regards to C_j expressed in a scale of 1 to 9 degrees (Table 7). In that scale, the values 1, 3, 5, 7, 9 mean equal, moderate, essential, demonstrated, extreme importance of one criterion with respect to another. The values 2,4,6,8 are of intermediate importance between the two adjacent judgments. For example, a value of 1 for a_{ij} means that criteria i and criteria j are both of the same importance.

The values of the resulting matrix A shown in Eq. 2 obey the scale of Saaty (Saaty 1994) and the values are based on personal judgment by 30 local experts, among researchers, engineers and practitioners. This mixed group give an initial idea of how important could be one criteria over others. For instance, it is assumed that the installation cost (C_5) is as important as the time of application (C_7) since both are directly related. In this case $a_{57} = a_{75}$ and both are 1. Additionally, mechanical ratio is considered as important as initial condition because both influence in the final result (greater reinforcement quantity greater load capacity or greater drift as initial condition greater damage in the strengthened wall which will affect the results). It is worth pointing out that seismic parameters as stiffness (C_1), strength (C_2) and ductility (C_3) are considered more important than the other criteria since they play a key role in the wall's performance and allow reducing the vulnerability associated to confined masonry buildings. This is why, for example, $a_{15} = 4$ or $a_{18} = 6$. The latter occurs with an exception of C_4 and C_{11}, and therefore $a_{41} = 2$ and $a_{11\,1} = 2$.

As a_{ij} depends on the relation w_i/w_j (w_i and w_j real weights of importance of the criteria C_i y C_j , respectively), the eigenvector W of A is formed by the sought weights w_1, w_2, ..., w_{11}, which are shown in Eq. 3. From Eq. 3 results that the C_4 (mechanical ratio) and C_{11} (initial test condition) criterion are more important with weight equal to 0.196; the criterion less important is C_8 (aesthetics) with weight $w_8 = 0.017$.

6.2 Ranking of the reinforcement alternatives

On the other hand, it must also take into account the yield x_{ij} of the i-th alternative (i = 1, 2, 3, 4, 5) in terms of the j-th criteria (j = 1, 2, ... , 11), which together make up the so-called decision matrix D = [x_{ij}] (Table 8). For C_1 the percentage of stiffness recovered was evaluated, for C_2 and

Table 7 Scale of relative importance Saaty (1994)

Intensity of Importance	Definition	Explanation
1	Equal importance	Two activities contribute equally to the objective
3	Moderate importance of one to another	Experience and judgment slightly favour one activity over another
5	Essential or strong importance	Experience or judgment strongly favours one activity over another
7	Demonstrated importance	An activity is strongly favoured and its dominance is demonstrated in practice
9	Extreme importance	The evidence favouring one activity over another is of the highest possible order of affirmation
2, 4, 6, 8	Intermediate values between the two adjacent judments	When compromise is needed
Reciprocal of above	If criterion i compared to j gives one of the above then j, when compared to i gives its reciprocal	

$$A = \begin{bmatrix} a_{11} & a_{12} & \cdots & a_{1\,11} \\ a_{21} & a_{22} & \cdots & a_{2\,11} \\ \vdots & \vdots & \ddots & \vdots \\ a_{11\,1} & a_{11\,2} & \cdots & a_{11\,11} \end{bmatrix} = \begin{bmatrix} 1 & 1 & 1 & 1/2 & 4 & 5 & 4 & 6 & 3 & 3 & 1/2 \\ 1 & 1 & 1 & 1/2 & 4 & 5 & 4 & 6 & 3 & 3 & 1/2 \\ 1 & 1 & 1 & 1/2 & 4 & 5 & 4 & 6 & 3 & 3 & 1/2 \\ 2 & 2 & 2 & 1 & 5 & 6 & 5 & 7 & 4 & 4 & 1 \\ 1/4 & 1/4 & 1/4 & 1/5 & 1 & 2 & 1 & 3 & 1/3 & 1/3 & 1/5 \\ 1/5 & 1/5 & 1/5 & 1/6 & 1/2 & 1 & 1/2 & 2 & 1/4 & 1/4 & 1/6 \\ 1/4 & 1/4 & 1/4 & 1/5 & 1 & 2 & 1 & 3 & 1/3 & 1/3 & 1/5 \\ 1/6 & 1/6 & 1/6 & 1/7 & 1/3 & 1/2 & 1/3 & 1 & 1/5 & 1/5 & 1/7 \\ 1/3 & 1/3 & 1/3 & 1/4 & 3 & 4 & 3 & 5 & 1 & 1 & 1/4 \\ 1/3 & 1/3 & 1/3 & 1/4 & 3 & 4 & 3 & 5 & 1 & 1 & 1/4 \\ 2 & 2 & 2 & 1 & 5 & 6 & 5 & 7 & 4 & 4 & 1 \end{bmatrix} \quad (2)$$

$$W = \{w_1, w_2, \ldots, w_{11}\} = \{0.125;\ 0.125;\ 0.125;\ 0.196;\ 0.033;\ 0.023;\ 0.033;\ 0.017;\ 0.063;\ 0.063;\ 0.196\} \quad (3)$$

Table 8 Decision Matrix

	C_1 [%]	C_2 [%]	C_3 [%]	C_4 [unit]	C_5 [%]	C_6 [%]	C_7 [days]	C_8 [mm]	C_9 [unit]	C_{10} [unit]	C_{11} [%]
WM	89	38	40	23.94	48	74	2.5	25	0.5	0.6	0.521
GFRP	57	3	0	12.93	32	46	1	0	0.7	0.7	0.769
CFRP	53	20	67	2.27	43	79	2	4	0.9	0.5	0.577
CSM	86	21	25	34.41	54	76	3	25	0.5	0.7	0.450
SRG	55	4	50	0.95	32	93	1	10	0.85	0.9	0.833

C_3 the increase in strength and ductility was evaluated against the original wall (see Section 4). C_4 points out the mechanical ratio presented in Section 4 as well. For C_5 and C_6 it was considered the percentage representing the cost of repairing and strengthening a damaged wall with against its construction cost (see Section 5). For C_7, indicates the days of delay in applying each technique (Section 5), for C_8 it was quantified the aesthetics, as the additional thickness that each technique adds to one side of the wall (Section 3.1). The durability to external agents C_9 and compatibility C_{10} were quantified by 30 local experts as was explained in Section 6.1. For instance, SRG is more durable in alkaline environment due to the lime-based mortar and steel cords that are galvanized. CFRP presents also a good performance in terms of durability (Gattesco and Boem 2017). SRG is more compatible with the masonry for its lime-based mortar with a low elastic modulus which matches that of the substrate. Conversely, the epoxy resin of CFRP is not compatible with the masonry. Finally, C_{11} indicates the final drift in tests of the non-reinforced wall (Section 3.3).

The first step of the ranking procedure is to normalize all x_{ij} values that have a different dimension. This normalization is carried out according to Eq. 4. The next step is to give weights to this matrix R (formed by r_{ij}) by multiplying each i-th column by the weight w_i of the i-th criterion, obtaining the matrix (5).

$$r_{ij} = \frac{x_{ij}}{\sqrt{\sum_{k=1}^{5} {x_{kj}}^2}} \quad (4)$$

The TOPSIS method indicates that the best alternative is

$$A = [v_{ij}] = [w_j r_{ij}] = \begin{bmatrix} 0.071 & 0.099 & 0.052 & 0.107 & 0.017 & 0.010 & 0.018 & 0.012 & 0.020 & 0.025 & 0.071 \\ 0.046 & 0.008 & 0.000 & 0.058 & 0.011 & 0.006 & 0.007 & 0.000 & 0.028 & 0.029 & 0.104 \\ 0.043 & 0.052 & 0.088 & 0.010 & 0.015 & 0.011 & 0.014 & 0.002 & 0.034 & 0.021 & 0.078 \\ 0.069 & 0.055 & 0.033 & 0.153 & 0.019 & 0.010 & 0.022 & 0.012 & 0.020 & 0.029 & 0.061 \\ 0.044 & 0.010 & 0.065 & 0.004 & 0.011 & 0.013 & 0.007 & 0.005 & 0.036 & 0.037 & 0.113 \end{bmatrix} \quad (5)$$

$$A^- = \{0.071; 0.099; 0.088; 0.004; 0.011; 0.006; 0.007; 0.000; 0.036; 0.037; 0.113\} \quad (6)$$

$$A^* = \{0.043; 0.008; 0.000; 0.153; 0.019; 0.013; 0.022; 0.012; 0.020; 0.021; 0.061\} \quad (7)$$

the one that has the least distance to the ideal solution A^* and the greater distance to the ideal negative solution A^-. The vector A^* is obtained by taking for each criterion the best performance value among A_1,.., A_5; the ideal negative solution A^- is composed of the worst performances.

If S_{i^*} and S_{i^-} are the Euclidean distances of the i-th alternative A_i from the ideal solutions and negative ideals A^* and A^-, respectively, the relative closeness C_{i^*} ($0 \leq C_{i^*} \leq 1$) of A_i with respect to the A^* it is defined as:

$$C_{i^*} = \frac{S_{i^-}}{S_{i^*} + S_{i^-}} \quad (8)$$

The final results are listed in Table 9. According to the TOPSIS method, the best option is the one with the greater C_{i^*} value. In this way, CFRP and SRG are the most suitable techniques, and it seems to be that the criteria C_4 and C_{11} strongly influences on these results. Both techniques have a low value of mechanical ratio and provide good results in terms of seismic parameters. In addition, it is evident that despite original SRG wall was failed (drift=0.833%) before the reinforcement process, this technique continues improving seismic parameters. Likewise, advantages related to SRG as durability and compatibility with masonry have led to rank SRG as a one of the most suitable seismic reinforcement.

Table 9 Relative closeness C_{i^*} of each alternative

WM	**A_1**	0.500
GFRP	**A2**	0.434
CFRP	**A3**	0.720
CSM	**A4**	0.267
SRG	**A5**	0.644

7. Conclusions

In Lima, the majority of buildings made with confined masonry walls is built without technical supervision, which results in informal dwellings. The inherent high seismic vulnerability of those buildings plus the fact that Peru is in a high seismic zone, results in a high seismic risk for the entire population. Therefore, there is the necessity to study a massive seismic reinforcement system that complies with many aspects such as economical, technical, among others for a mass use plan. The studied reinforcing techniques were Welded Mesh System (WM), Glass and Carbon Fiber Reinforced Polymer (GFRP and CFRP), Deformed Steel Meshes (CSM) and Steel Reinforced Grout (SRG). The experimental tests, carried out by some researchers at the PUCP, consisted to apply an in-plane cyclic loading on some typical confined masonry walls but strengthened with the different reinforcement options. The strengthening of confined masonry through traditional (WM, CSM) or innovative (GFRP, CFRP, SRG) techniques presented interesting aspects and results have been pointed out.

For example, looking at the recovery of the initial stiffness, theWMand CSM recovered approximated an 87% of that, but part of thiswas due to the repair process and the remainingwas due to the increasing of the wall?s thickness in 50 mm provided by both techniques. In case of GFRP, CFRP and SRG, a stiffness recovering of approximated 55% was computed, which can be attributed almost in total to the repair process since these techniques almost did not increase wall?s thickness. However, not only a fully recovery of the initial stiffness is a guarantee of a good seismic behavior, it is also necessary to recover the maximum wall load capacity and to look for an increment of the displacement ductility. In this case, all reinforcement options, except the GFRP, showed to fulfil these conditions.

Just the WM and CSM covered completely all the walls, which means to require more quantity of reinforcement compared with the other ones. In the case of GFRP, CFRP and SRG, the reinforcement just required to be placed on some horizontal wall zones. The walls with WM and CSM allowed to have smeared cracking in the walls along the tests. In comparison, the other systems just controlled the thickness of previous cracks also after the maximum wall load capacity; then, new cracks appeared and the same time that reinforcement system started to break at some points. In addition, it is important to look also for the facility of the reinforcement installation thinking on a mass application. In this case, the SRG, followed by the CFRP, is the one with an easy a fast application.

Finally, the economy of the population have been taken account in order to propose a type of reinforcement among the five aforementioned for a mass use plan. This study is an effort towards it and presents how the MCDM method is effective for the decision making. The applied TOPSIS

method allowed the qualification of the performance of each alternative through 10 criteria, which are not only related to the improvement of seismic-resistant parameters but also cost-effectiveness. Another criteria were also taken into account as the reinforcement configuration by means of mechanical ratio, the duration of application, aesthetics, durability, compatibility, and the initial test condition.

Among the five presented options and the indicated criteria, the best solutions turn out to be the Carbon Fiber Reinforced Polymer (CFRP) and Steel Reinforced Grout (SRG). Hence, CFRP and SRG are the reinforcements of massive, fast and effective application. Likewise, it is important to mention that it is not necessary to reinforce all the walls of a building. In case of cracked walls, it is evident that they were major structural elements so they must be repaired and strengthened. In case of new buildings or without structural damage, a technical evaluation must be carried out in order to identify the main structural elements. However, the proper training of the people in charge of the application of these reinforcement systems is highly recommended.

Acknowledgments

This project was partially funded by CONCYTEC within the framework of the N-232-2015-FONDECYT Agreement. The authors would like to acknowledge the important collaboration of the industrial company Kerakoll S.p.A., especially Dr Paolo Casadei, for providing the materials for the experimental part of the walls strengthened with SRG. Additonally, thanks to MSc. Alfredo Manchego for his important contribution to the development of these project.

References

Ahmad, N., Crowley, H., Pinho, R. and Ali, Q. (2010), "Displacement-based earthquake loss assessment of masonry buildings in Mansehra city, Pakistan", *Journal of Earthquake Engineering*, **14**(1), 1-37.

Alcocer, S., Arias, J. and Vazquez, A. (2003), "The new Mexico City building code requirements for design and construction of masonry structures", *Proc Ninth North American Masonry Conference, Clemson, South Carolina*, 656-667.

Bhattacharya, S., Nayak, S. and Chandra, S. (2013), "A critical review of retrofitting methods for unreinforced masonry structures", *International Journal of Disaster Risk Reduction*, 51-67.

Brzev, S. and Perez, J. (2014), "Masonry Construction around the world: an overview", *Short Course on Seismic Design of Reinforced and Confined Masonry Buildings*.

Buchan, P. and Chen, J. (2007), "Blast resistance of FRP composites and polymer strengthened concrete and masonry structures: A state of the art review", *Composites Part B: Engineering*, **38**, 509-522.

Cabral-Fonseca, S., Correia, J.R., Custódio, J., Silva, H.M., Machado, A.M. and Sousa, J. (2018), "Durability of FRP - concrete bonded joints in structural rehabilitation: A review", *International Journal of Adhesion and Adhesives*, **83**, 153 - 167.

Carloni, C. (2017), "Prove di compressione diagonale per la valutazione dell'efficacia di rinforzi strutturali applicati su pannelli murari di laterizio e malta di calce. Convenzione di ricerca con kerakoll spa rapporto di prova", *Universita di Bologna*.

Caterino, N., Iervolino, I., Manfredi, G. and Cosenza, E. (2006), "Multi-criteria decision making for seismic retrofitting of an underdesigned RC structure", *First European Conference on Earthquake Engineering and Seismology (a joint event of the 13th ECEE 30th General Assembly of the ESC), Geneva, Switzerland*.

Corradi, M., Borri, A. and Vignoli, A. (2002), "Strengthening techniques tested on masonry structures struck by the Umbria–Marche earthquake of 1997–1998", *Composites Part B: Engineering*, **16**, 229–239.

De Santis, S., Ceroni, F.G., De Felice, G., Fagone, M., Ghiassi, B., Kwiecie, A., Lignola, G.P., Morganti, M., Santandrea, M., Valluzzi, M.R. and Viskovic, A. (2017), "Round Robin Test on tensile and bond behavior of Steel Reinforced Grout systems", *Composites Part B: Engineering*, **127**, 100 - 120.

FEMA. (2009), "Unreinforced Masonry Buildings and Earthquakes: Developing Successful Risk Reduction Programs", *Federal Emergency Management Agency*.

Gattesco, N. and Boem, I. (2017), "Characterization tests of GFRM coating as a strengthening technique for masonry buildings", *Composite Structures*, **165**, 209–222.

Ghiassi, B., Oliveira, D., Marques, V., Soares, E. and Maljaee, H. (2016), "Multi-level characterization of steel reinforced mortars for strengthening of masonry structures", *Journal Materials Design*.

Hwang, C.L. and Yoon, K. (1981), "Multiple Attribute Decision Making", *Lecture Notes in Economics and Mathematical Systems*.

INEI (2017), "Perfil sociodemográfico del Perú: Censos Nacionales 2007: XI de población y VI de vivienda".

Lodi, S., Alam, N. and Ahmed, M. (2014), "Seismic Vulnerability Assessment of Existing Buildings of Pakistan, Earthquake Model for Middle East Region (EMME)", *Department of Civil Engineering, NED University of Engineering & Technology, Karachi, Pakistan*.

Lovon H., Tarque N., Silva V. and Yepes-Estrada, C. (2018), "Development of Fragility Curves for Confined Masonry Buildings in Lima, Peru", *Earthquake Spectra*, **34**(3), 1339-1361.

Lujan, M. (2016), "Refuerzo de muros de albañilería confinada con mallas de acero", *Bachelor Thesis. School of Science and Engineering. Pontificia Universidad Catolica del Peru, Lima, Peru*.

NTP E.070. (2006), "Reglamento Nacional de Edificaciones: Albañilería", *Ministerio de Vivienda, Construcción y Saneamiento - SENCICO*.

Popa, V., Pascu, R., Papurcu, A. and Albota, E. (2016), "Retrofitting of squat masonry walls by FRP grids bonded by cement-based mortar", *Earthquakes and Structures*, **10**(1), 125-139.

Remki, M., kehila, F., Bechtoula, H. and Bourzam, A. (2016), "Seismic vulnerability assessment of composite reinforced concrete-masonry building", *Earthquakes and Structures*, **11**(2), 371-386.

Salsavilca, J., Yacila, J. and Tarque, N. (2019), "Aplicación de la Fibra de Acero Galvanizado para el Reforzamiento Estructural de Muros de Albañilería Confinada ante Cargas Cíclicas en su Plano ", *MSc. Thesis. Civil Engineering Department. Pontificia Universidad Católica del Perú, Lima, Peru*.

San Bartolomé, A. and Castro, A. (2002), "Reparación de un muro de albañilería confinada mediante malla electrosoldada", *Internal Report, Civil Eng. Division. School of Science and Engineering. Pontificia Universidad Católica del Perú, Lima, Peru*.

San Bartolomé, A., Castro, A., Vargas, B. and Quiun, D. (2008), "Repair of reinforced masonry walls with shear failure", *14th*

International Brick and Block Masonry Conference, Sydney, Australia, in CDROM, February 2008.

San Bartolomé, A. and Loayza, J. (2004), "Reparación y reforzamiento con varillas de fibra de vidrio en un muro de albañilería confinada", *Internal Report, Civil Eng. Division. School of Science and Engineering. Pontificia Universidad Católica del Perú, Lima, Peru*.

San Bartolomé, A. and Coronel, C. (2009), "Reparación y reforzamiento de un muro de albañilería confinada mediante fibra de carbono", *Internal Report, Civil Eng. Division. School of Science and Engineering. Pontificia Universidad Católica del Perú, Lima, Peru*.

Saaty, T. (1994), "How to Make a Decision: The Analytic Hierarchy Process", *INTERFACES*, **24**(6), 19–43.

Smyrou, E. (2015), "FRP versus traditional strengthening on a typical mid-rise Turkish RC building", *Earthquakes and Structures*, **9**(5), 1069-1089.

Srechai, J., Leelataviwat, S., Wongkaew, A. and Lukkunaprasit, P.(2017), "Experimental and analytical evaluation of a low-cost seismic retrofitting method for masonry-infilled non-ductile RC frames", *Earthquakes and Structures*, **12**(6), 699-712.

Yacila, J., Salsavilca J., Tarque, N., Casadei P. and Camata, G. (2019), "The use of SRG to improve the lateral displacement ductility of confined masonry walls", Proceedings of the 13NAMC, paper number 048.